DOI: 10.21062/mft.2022.088  http://www.journalmt.com

# Structural Optimization of Small-Diameter Deep Well Rescue Robot based on Hyperworks-Optistruct

Yi Zheng (0000-0002-7853-8279)[1], Zhe Wu (0000-0002-8800-5281)[1,2], Chao Ma (0000-0002-9332-3866)[1,2]
[1]Institute of Intelligence and Manufacture, Qingdao Huanghai University, No. 1145 Linghai Road, Huangdao District, Qingdao, 266427, China. E-mail: fw.2004@163.com
[2]College of mechanical and electrical automotive engineering, Yantai University, No. 30, Qingquan Road, Laishan District, Yantai, 264005,China.1806967361@qq.com,565828320@qq.com

**This paper aims to solve the problems related to poor motion continuity and the abrupt acceleration of a small-diameter deep well rescue robot in the process of motion characteristics analysis. According to the movement characteristics and the structural forms of the grasping mechanism and the bracket mechanism of the deep well rescue robot, the finite element analysis of the key mechanism is carried out based on the Hyperworks-Optistruct solver. According to the analysis results, the specific parameters to be optimized are obtained. Moreover, the topology optimization of the key mechanism is carried out, and the optimal design scheme of the clamping mechanism and the bracket mechanism of the deep well rescue robot are obtained. The optimization results show that, on the premise of meeting the strength requirements, the grid density distribution law is obtained. According to the variation law of the lightweight curve, the overall weight of the grasping mechanism and the bracket mechanism decreases obviously. The whole optimization process is completed, and the final optimization result is obtained.**

**Keywords:** Small diameter robot; Deep well rescue robot; Structure optimization; HyperWorks

## 1 Introduction

The condition of the small-diameter deep well is special, and the requirement for a deep well rescue robot is high. The rescue robot must maintain the continuity of motion and the stability of the system while moving on the shaft wall, gripping the grasping mechanism, and lifting the bracket mechanism. Through kinematic and dynamic analysis, it has been found that, when performing the above actions, the rescue robot system will have fluctuations and discontinuities of some key actions and abrupt changes in acceleration are also encountered[1-2]. In order to improve the efficiency of the whole mechanism, the structure of the grasping and the bracket mechanisms are further optimized[3].

Therefore, Hyperworks software integrates an open architecture and a programmable workbench to provide state-of-the-art CAE modeling, visualization analysis, and optimization analysis, as well as robustness analysis, multi-body simulation, manufacturing simulation, and process automation. Moreover, OptiStruct is the preeminent finite element structural analysis and optimization software with an accurate and fast finite element solver for conceptual design and refinement. Using a library of standard cells and various boundary condition types, users can perform linear static and natural frequency optimization analyses[4-6].

During the process of optimization design, the operation is simple, and the tedious programming process is avoided. The structural optimization can be realized through the command window setting and post-processing. Therefore, in this paper, through Hyperworks' Optistruct solver software, the grasping and the bracket mechanisms of the deep well rescue robot are optimized[7-8].

## 2 Optimization of key institutional structure

The optimization of the key institutional structure consists of five phases that will be presented here below:

### 2.1 Mathematical model establishment of the grasping mechanism

For the convenience of calculation, a simplified model is established, based on the grasping mechanism structure, as shown in Fig. 1. With the electric lead rod as the center, the center point is set as point *C* whereas *G* is the highest point of the upward movement of the open frame and *O* indicates the lowest point when the frame moves down.

Let the distance CD between the center point *C* and the connection point *D* between the right clamping arm and the front frame be $x_1$ (measured in mm). Moreover, GH represents the distance between the highest point *G* of the bracket moving upward and the connecting point *H* (between the bracket and the right connecting rod) that is set to $x_2$. The distance HI

between the connecting point *H* and the connecting point *I* (between the right connecting rod and the right clamping arm) is $x_3$. Furthermore, let the distance DI between the connection points *D* and *I* be $x_4$ and the distance DM between the connection point D and the lower endpoint *M* of the right bracket opening frame be $x_5$. Added to that, the distance between the contact point *L* of the right steering drive wheel and the grabbed object and the lower endpoint *M* of the right bracket under the clamping state is $x_6$ . Finally, the angle DML value is represented by $x_7$ (measured in degrees). Therefore, the design variables of the grasping mechanism are:

$$X = \left[x_1, x_2, x_3, x_4, x_5, x_6, x_7\right]^T \tag{1}$$

## 2.2 Establishment of the mathematical model of mechanical constraint

Fig. 1 shows the force analysis diagram of the grasping mechanism. Driven by the electric lead rod, the maximum distance CG is equal to 0.07 m for the open frame to move up and down whereas the radius of the grasping working space is equal to 160 mm, and the distance from the center point to the lower surface of the front frame is equal to 210 mm. The force equations of the deep well rescue robot during its movement on the inner wall of the deep well can be expressed as follows:

$$M_c(F') = -DS \cdot F' = x_4 \sin \angle DIH \cdot F' \tag{2}$$

$$\angle DIH = \arccos\left[\frac{x_3^2 + x_4^2 - CG^2 - (x_1 - x_2)^2}{2x_3x_4}\right] \tag{3}$$

$$F' = \frac{F}{2\sin \angle HIO} \tag{4}$$

$$\angle HIO = \arctan\frac{GO}{x_1 - x_2} \tag{5}$$

$$M_c(F_N) = DP \cdot F_N = x_5 \sin x_7 \cdot F_N \tag{6}$$

Where F is the rated tension of the electric lead rod (measured in N), F' is the force exerted on point I (measured in *N*), and $F_N$ is the pressure applied on the clamping point *M* of the clamping arm when the clamping arm is tightened (measured in *N*). Moreover, $M_c(F')$ is the torque of tension on point *D* when the clamping arm is tightened (measured in N·mm) and $M_c(F_N)$ is the torque generated by the pressure $F_N$ between the clamping point *M* to point *D* when the clamping arm is tightened (measured in N·mm).

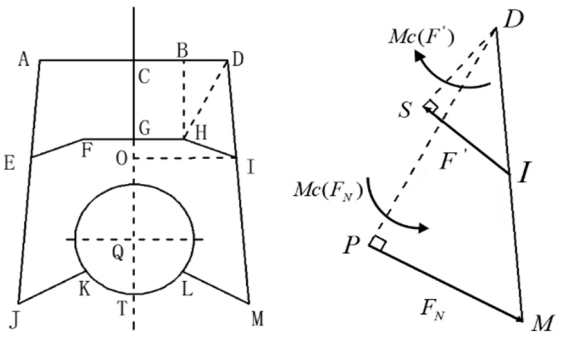


***Fig. 1*** *Structure of the grasping mechanism and the force analysis model*

## 2.3 Establishment of the geometric dimension constraint mathematical model

During the movement of the deep well rescue robot, the installation space of each component should be complete, and non-interference should be ensured, especially for the grasping mechanism. The clamping arms on both sides should not collide with each other when clamping[9-10]. Thus, combined with other components of the deep well rescue robot, the geometric constraints are established as follows (all variables are measured in mm except $x_7$ that is measured in degrees):

$$\begin{aligned} x_1 &\in [135,145] \\ x_2 &\in [15,20] \\ x_3 &\in [125,135] \\ x_4 &\in [123,128] \\ x_5 &\in [327,332] \\ x_6 &\in [145,150] \\ x_7 &\in [40,50] \end{aligned} \tag{7}$$

In view of the system requirements, it is also necessary to meet the following constraints:

$$x_2 + x_3 > x_1 \tag{8}$$

$$x_4 < x_5 \tag{9}$$

$$60^\circ \le \angle DIH \le 90^\circ \tag{10}$$

$$\angle BDI > 60^\circ \tag{11}$$

The Angle between the two clamping arms should be 120°, so ∠KQT should be between 55° and 65°. Thus, the formula is as follows:

$$55^\circ \le \arctan\frac{\sqrt{x_5^2 + x_6^2 - 2x_5x_6\cos x_7}\cdot\cos(\alpha+\beta-\chi) - x_1}{-0.22 + \sqrt{x_5^2 + x_6^2 - 2x_5x_6\cos x_7}\cdot\sin(\alpha+\beta-\chi)} \le 65^\circ \tag{12}$$

Where α, $\beta$, and $\chi$ represent, respectively, the angles ∠IDH, ∠JCL, and ∠MDL.

When the frame is open and the two frame rods are in a straight line, the horizontal distance of the center point of the steering drive to the pipeline should be greater than 160mm and the formula is as follows:

$$\sqrt{x_5^2+x_6^2-2x_5x_6\cos x_7}\cdot\sin(\alpha-\angle IDL)+x_1\le 80 \tag{13}$$

### 2.4 Establishment of objective function

According to the electric lead rod, when the clamping arm is tightened, the maximum pressure of the steering drive wheel on the surface of the pipeline represents the objective function that is expressed as follows:

$$F_1(x)=\frac{F}{F_N}=\frac{(x_6-x_5\cos x_7)2\sin\angle HIO}{x_4\sin\angle DIH} \tag{14}$$

The components should be as compact as possible, so:

$$F_2(x)=\sum_{i=1}^{6}x_i \tag{15}$$

This yields in obtaining the final objective function as follows:

$$f(x)=\min\left[F_1(x)+F_2(x)\right]=\min\left[\frac{(x_6-x_5\cos x_7)2\sin\angle HIO}{x_4\sin\angle DIH}+\sum_{i=1}^{6}x_i\right] \tag{16}$$

#### 2.4.1 Size determination

*Fminocon ()* function is used to analyze and calculate the size of the clamping arm[11-13]. It can be expressed as follows:

$$\min f(x)\begin{cases}Ax\le B\\ A_{eq}x=B\\ x_m\le x\le x_M\\ C(x)\le 0\\ C_{eq}=0\end{cases} \tag{17}$$

This function is called using the below parameters:

$$\left[x,f_{opt},flag,c\right]=f\min con(F,x_0,A,B,A_{eq},B_{eq},x_m,x_M,CF,OPT) \tag{18}$$

Where $F$ is the objective function, $CF$ is an $M$ file written by nonlinear constraint functions, $X$ is the design variable, OPT is the control option and $f_{opt}$ is the optimization result of objective function[14-16]. After calculation, the output parameters are the seven variables of vector $X$ defined in Eq. (1). Finally, the size calculation results of the grasping mechanism are shown in Table 1.

***Tab. 1*** *Clamping arm dimension parameters*

| Parameter | $x_1$ | $x_2$ | $x_3$ | $x_4$ | $x_5$ | $x_6$ | $x_7$ |
|---|---|---|---|---|---|---|---|
| size | 140mm | 19mm | 134mm | 125mm | 330mm | 148mm | 45° |

## 3 Optimization design analysis of grasping mechanism

The finite element analysis method is adopted to carry out model discretization and mesh division for the gripping mechanism[17-18]. Through the Optistruct solver, the material of the gripping mechanism is defined to be the aluminum alloy and the effect after choosing it is shown in Fig. 2.

Moreover, the constraints have been defined and the boundary conditions have been implemented as shown in Fig. 3.

After the above preparations are made, simulation parameters are set to simulate and analyze the motion results of the gripping mechanism. The reaction force is shown in Fig. 4.

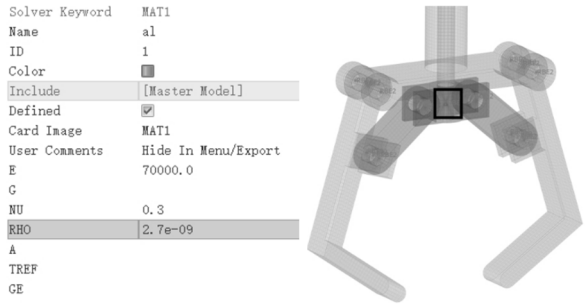


***Fig. 2*** *Parameter enactment of the gripper*

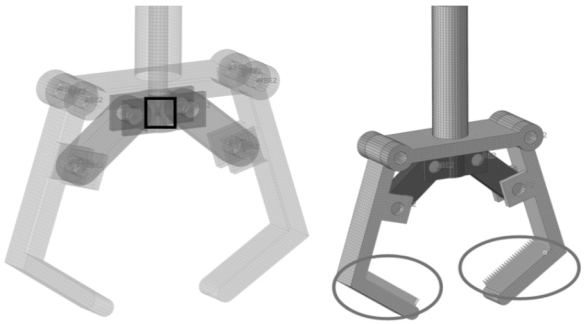

***Fig. 3*** *Adding constraints and load to the gripper model*

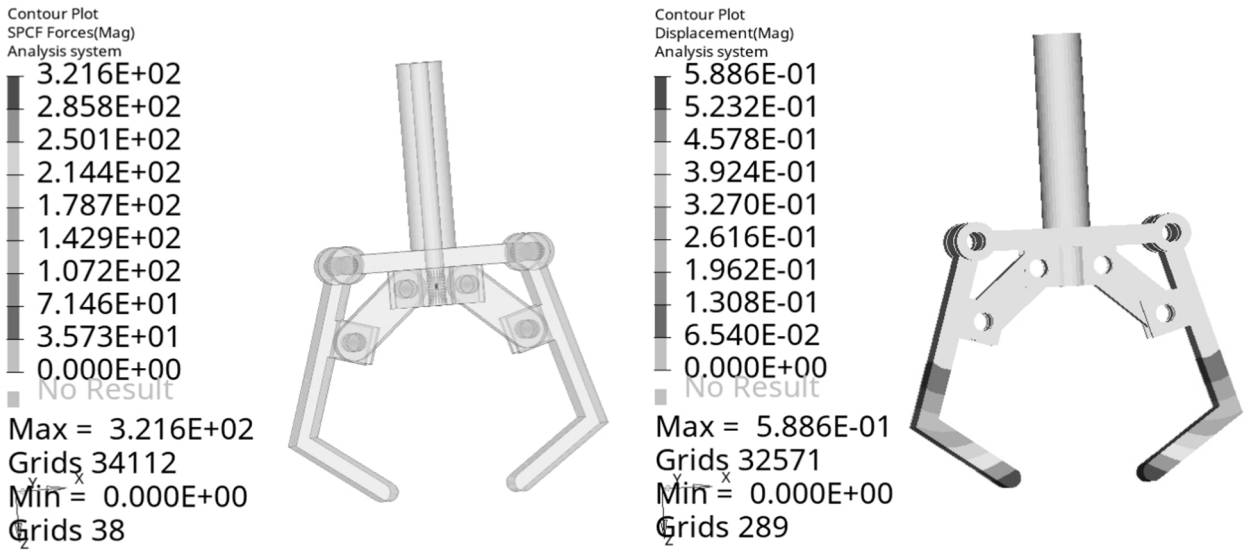


***Fig. 4*** *Effect of the gripping mechanism reaction*

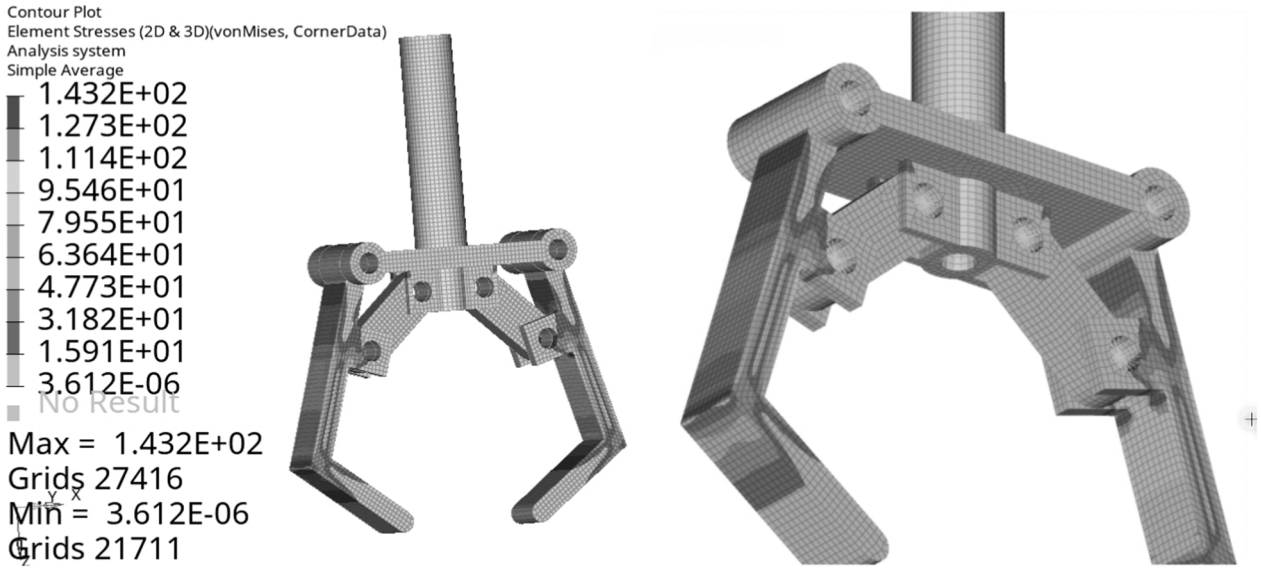


***Fig. 5*** *Effect of stress on the gripping mechanism*

Finally, the acting stress of the gripping mechanism is shown in Fig. 5.

Referring to Fig. 4, there is a large reaction force at the tip of the gripping mechanism and at the connection point between the push-pull rod and the push-pull part. As for Fig. 5, there is a relatively large force under the connecting ear of the gripping mechanism.

Moreover, there is a local red dense area and a stress concentration [19-20]. Therefore, in the process of optimization, it is necessary to reduce the influence of the reaction force and the stress concentration. Thus, the structure of the gripping mechanism is optimized, and the optimization results are shown in Fig. 6.

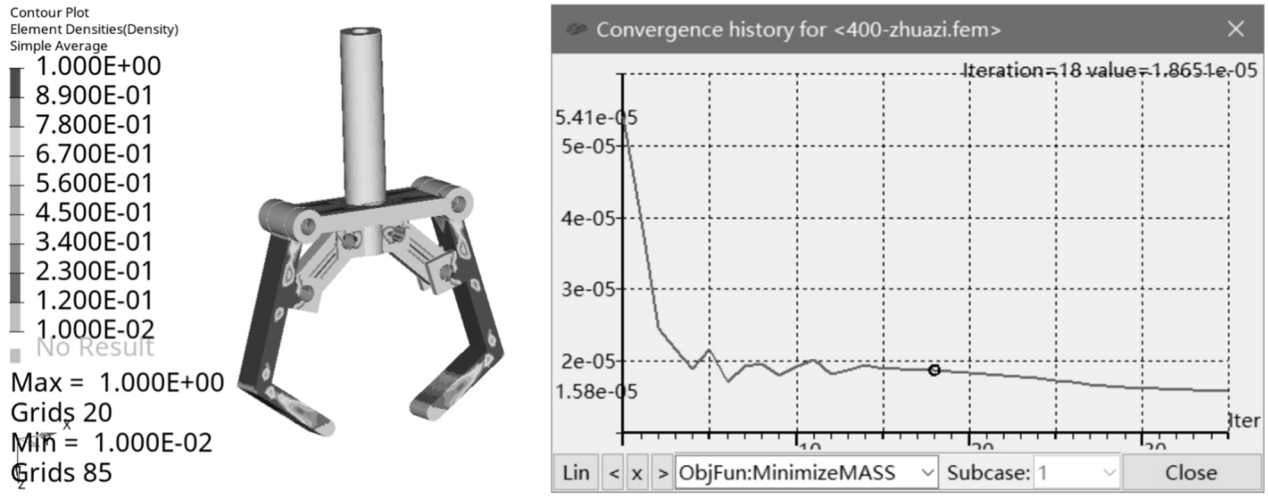


***Fig. 6*** *Optimization results of the gripping mechanism*

Through the mesh division of the gripping and the bracket mechanisms, the definition of materials and their properties has been proposed. During the movement of the mechanism, the motion boundary conditions are set as well as the constraints between the moving parts. Then, the loads are added and the simulation analysis is conducted. Moreover, the position with relatively large reaction force and the phenomenon of stress concentration are obtained and the location of stress concentration is determined. Therefore, the goal of optimizing the grip and the bracket mechanisms is to reduce the reaction force and limit the influence of stress concentration on the motion of the gripper mechanism [21-22]. After ensuring the above optimization analysis, the overall weight optimization result of the small-caliber deep well rescue robot is shown in Fig. 6. According to the variation of the lightweight curve, the overall weight of the small-caliber deep well rescue robot decreases significantly, therefore meeting the design requirements.

## 4 Conclusion

Aiming at the problems of small working space and difficult rescue of small-caliber deep well rescue robot, and in order to increase the movement flexibility of the robot during rescue, a mathematical model representing the motion of small-caliber deep well rescue robot grasping and bracket mechanisms is established, and the function of motion and target variables is designed. The optimal design and the analysis of the gripping and the bracket mechanisms were carried out and the positions and the needed parameters to achieve optimization. According to the relevant parameters, the density distribution of the key mechanism is set. Moreover, the optimization results show that there is a large reaction force and stress concentration in the tip of the gripping mechanism, the connection between the push and pull rod, and the push and pull parts which are the first positions to be optimized. As the bracket mechanism consists of four parts with a 90 degrees interval distribution, there is also a large reaction force and stress concentration at the tip of the bracket and the inclined tie rod. After realizing the optimization design, the lightweight change curve of the deep well rescue robot with lower caliber is obtained. From the variation track of the lightweight curve, it can be seen that the overall weight decreases significantly when the functional application requirements are met, and the purpose of structure optimization is achieved.

## Acknowledgements

***Qingdao postdoctoral applied research project (A2020-070). The Natural Science Foundation of Shandong Province (No.ZR2020QE151) and Qingdao Huanghai University doctoral research Fund Project (2020boshi02).***

## References

[1] GAYATHIRI, R., NALINI, M., ARCHANA, R., NAMBIAR, M. V., KISHORE, S. (2021). Hand gesture base bore well rescue robot. In: *Materials Today: Proceedings*, Vol. 46, No. 9, pp. 4203-4206. ISSN 2214-7853

[2] JAN, K., KRISTINA, B., OLEKSANDR, P., NADIIA, A. (2022). Erosion Modelling of Structural Materials in the Working Space of Multistage Convective Dryers.In: *Manufacturing Technology*, Vol. 22, No. 4, pp. 307-318. ISSN: 1213-2489

[3] MASATOSHI, H., TOSHIFUMI, FUJII. (2020). 3-d shape recognitions of target objects for stacked rubble withdrawal works performed by rescue robots. In: *Artificial Life and Robotics*, Vol. 25, No. 1, pp. 94-99. ISSN 1433-5298

[4] PAVOL, T., TATIANA, C., ANDREJ, C., SILVIA, S., JOZEF, H., MIROSLAV, C. (2022). Analysis of Parameters of Sintered Metal Components Created by ADAM and SLM Technologies. In: *Manufacturing Technology*, Vol. 22, No. 4, pp. 347-355. ISSN: 1213-2489

[5] ALATISE, M. B., HANCKE, G. P. (2020). A Review on Challenges of Autonomous Mobile Robot and Sensor Fusion Methods. In: *IEEE Access*, Vol. 8, pp. 39830-39846. ISSN 2169-3536

[6] JALEEL, H., SHAMMA, J. S. (2020). Distributed optimization for robot networks: from real-time convex optimization to game-theoretic self-organi zation. In: *Proceedings of the IEEE*. Vol. 108, No. 11, pp. 1953-1967. ISSN 0018-9219

[7] TUONG N. V., NAPRSTKOVA, N. (2019). Matlab-based Calculation Method for Partitioning a Free-form Surface into Regions. In: *Manufacturing Technology*, Vol. 19, No.3, pp. 518-524. ISSN: 1213-2489

[8] TIAN, Y., LIU, K., OK, K., TRAN, L., HOW, J. P. (2020). Search and rescue under the forest canopy using multipleuas. In: *The International Journal of Robotics Research*, Vol. 39, No. 10, pp. 1201-1221. ISSN 0143-991X

[9] LIAO Y. Y. , LIAO B. Y. (2021).Lightweight Design and Optimization Effect Evaluation of Hydro Generator Set. In: *Manufacturing Technology*, Vol. 21, No.2, pp. 223-230. ISSN: 1213-2489

[10] SHI,Y. D., HE,W., GUO,M.Q., XIA, D., LUO,X., JI,X.Q. (2022). Mechanism Design and Motion Analysis of a Flapping-Wing Air Vehicle. In: *Mathematical Problems in Engineering*, Hindawi, Vol. 2022, pp. 1-11. ISSN 1024-123X

[11] WOLEK, A., CHENG, S., GOSWAMI, D., PALEY, D. A. (2020). Cooperative mapping and target search over an unknown occupancy graph using mutual information. In: *IEEE Robotics and Automation Letters*, Vol. 5, No. 2, pp. 1071-1078. ISSN 2377-3766

[12] XU, W., PAN, E., LIU, J., LI, Y., YUAN, H. (2021). Flight control of a large-scale flapping-wing flying robotic bird: system development and flight experiment. In: *Chinese Journal of Aeronautics*, Vol. 35, No. 2, pp. 235-249. ISSN 1000-9361

[13] TETSUSHI K., TAICHI A., SATOSHI S.(2020). Development of a separable search-and-rescue robot composed of a mobile robot and a snake robot. In: *Advanced Robotics*, Vol. 34, No. 2, pp. 132-139. ISSN 0169-1864

[14] GOUGH, E., CONN, A., ROSSITER, J. (2021). Planning for a tight squeeze:navigation of morphing soft robots in congested environments. In: *IEEE Robotics and Automation Letters*, Vol. 6, No. 3, pp. 4752-4757. ISSN 2377-3766

[15] PAN, E., LIANG, X., XU, W. (2020). Development of vision stabilizing system for a large-scale flapping-wing robotic bird. In: *IEEE Sensors Journal*, Vol. 20, No. 14, pp. 8017-8028. ISSN 1530-437X

[16] MUNTWILER, S., WABERSICH, K. P., CARRON, A., ZEILINGER, M. N. (2020). Distributed model predictive safety certification for learning-based control. In: *IFAC-Papers On-Line*, Vol. 53, No. 2, pp. 5258-5265. ISSN 2405-8963

[17] GAO, Z., QIN, J., WANG, S., WANG, Y. (2021). Boundary gap based reactive navigation in unknown environments. In: *Journal of automation: English edition*, Vol.8, No. 2, pp. 468-477. ISSN 2329-9266

[18] TSENG, K. S., METTLER, B. (2020). Analysis and augmentation of human performance on telerobotic search problems. In: *IEEE Access*, Vol. 8, pp. 56590-56606. ISSN 2169-3536

[19] DUCA, R. N., BUGEJA, M. K. (2020). Multi-robot energy-aware coverage control in the presence of time-varying importance regions. In: *IFAC-Papers OnLine*, Vol. 53, No. 2,pp. 9676-9681. ISSN 2405-8963

[20] SHREE, V., ASFORA, B., ZHENG, R., HONG, S., CAMPBELL, M. (2021). Exploiting natural language for efficient risk-aware multi-robot sar planning. In: *IEEE Robotics and Automation Letters*, Vol. 6, No. 2,pp. 3152-3159. ISSN 2377-3766

[21] WILLIAMS, D., KHODAPARAST, H. H., JIFFRI, S. (2021). Active vibration control of an equipment mounting link for an exploration robot. In: *Applied Mathematical Modelling*, Vol. 95, No. 6,pp. 524-540. ISSN 0307-904X

[22] ANYFANTIS, A., SILIS, A., BLIONAS, S. (2021). A low cost, mobile e-nose system with an effective user interface for real time victim localization and hazard detection in user operations. In: *Measurement: Sensors*, Vol. 16, No. 2,pp. 100049. 2665-9174